Enhanced pyroelectric property in (1x)(Bi0.5Na0.5)TiO3-xBa(Zr0.055Ti0.945)O3: Role of morphotropic phase boundary and ferroelectric-antiferroelectric phase transition

Feifei Guo, Bin Yang, Shantao Zhang, Fengmin Wu, Danqing Liu, Pingan Hu, Ye Sun, Dali Wang, and Wenwu Cao

Citation: Applied Physics Letters **103**, 182906 (2013); doi: 10.1063/1.4828675
View online: http://dx.doi.org/10.1063/1.4828675
View Table of Contents: http://scitation.aip.org/content/aip/journal/apl/103/18?ver=pdfcov
Published by the AIP Publishing

Enhanced pyroelectric property in $(1-x)(Bi_{0.5}Na_{0.5})TiO_3$-$xBa(Zr_{0.055}Ti_{0.945})O_3$: Role of morphotropic phase boundary and ferroelectric-antiferroelectric phase transition

Feifei Guo,[1] Bin Yang,[1,a)] Shantao Zhang,[2,b)] Fengmin Wu,[1] Danqing Liu,[3] Pingan Hu,[4] Ye Sun,[1] Dali Wang,[3] and Wenwu Cao[1,5]
[1]*Condensed Matter Science and Technology Institute, Harbin Institute of Technology, Harbin 150080, China*
[2]*National Laboratory of Solid State Microstructures and Department of Materials Science and Engineering, Nanjing University, Nanjing 210093, China*
[3]*School of Chemical Engineering and Technology, Harbin Institute of Technology, Harbin 150080, China*
[4]*School of Materials Science and Engineering, Harbin Institute of Technology, Harbin 150080, People's Republic of China*
[5]*Materials Research Institute, The Pennsylvania State University, University Park, Pennsylvania 16802, USA*

(Received 8 May 2013; accepted 19 October 2013; published online 1 November 2013)

$(1-x)(Bi_{0.5}Na_{0.5})TiO_3$-$xBa(Zr_{0.055}Ti_{0.945})O_3$ ($0 \le x \le 0.12$) lead-free ceramics have been prepared and the morphotropic phase boundary (MPB) is confirmed to be $x = 0.06$–0.09. The MPB composition $x = 0.07$ shows enhanced pyroelectric properties from room temperature (RT) to the depolarization temperature T_d (87 °C), with the pyroelectric coefficient $p = 0.057\ \mu C/cm^2\,°C$ and the figures of merit $F_i = 203$ pm/V, $F_v = 0.022\ m^2/C$, and $F_d = 10.5\ \mu Pa^{-1/2}$ at RT and the highest pyroelectric coefficient of $2.21\ \mu C/cm^2\,°C$ near T_d. These values are superior to other lead-based/lead-free pyroelectric ceramics. Enhanced pyroelectric properties can be explained by the effects of MPB and ferroelectric-antiferroelectric phase transition. © *2013 AIP Publishing LLC*. [http://dx.doi.org/10.1063/1.4828675]

Pyroelectric detectors made of ferroelectric (FE) materials have become the most widely used infrared detectors due to their simple design and high performance. There are two main classes of ferroelectric ceramics that have been used for pyroelectric detectors. One is based on ceramics such as $Ba_{1-x}Sr_xTiO_3$ (BST), $Pb(Sc_{1/2}Ta_{1/2})O_3$ (PST), and $(Pb_{0.832}Ba_{0.138}La_{0.02})(Zr_{0.7}Ti_{0.05}Sn_{0.25})O_3$ (PLBZST). Strong pyroelectric effect can be generated around the ferroelectric-antiferroelectric (AFE)/paraelectric phase transition; therefore, such detectors should be operated near the phase transition temperature. Temperature stability is often a key concern for these pyroelectric ceramics. In addition, the pyroelectricity in these materials must be stabilized by a dc bias, which also limits the device performance.[1,2] The other class is the conventional pyroelectric ceramics, such as $Pb(Zr,Ti)O_3$ (PZT) and $PbMg_{1/3}Nb_{2/3}O_3$-$PbTiO_3$ (PMN-PT), with composition around the morphotropic phase boundary (MPB), such detectors can be operated well below the Curie temperature (T_c) using poled ferroelectric materials; the pyroelectric response of these materials is reversible and stable.[3,4] Although this kind of detectors can be operated well below T_c without a bias field, temperature stabilizers are required in practical applications, and these class of materials are mainly lead-containing compounds. With increasing environmental concerns, some countries already started to restrict the use of lead-containing materials. In recent years, intense research has been conducted in searching for lead-free pyroelectric materials to replace those widely used lead-containing materials.[5]

Lead-free $Bi_{0.5}Na_{0.5}TiO_3$ (BNT) ceramic can form solid solution, which not only has a MPB similar to that of PZT but also has a ferroelectric-antiferroelectric phase transition around the depolarization temperature ($T_d \sim 160$ °C for pure BNT); both are advantageous for improving pyroelectric performance. In other words, BNT-based solid solutions with MPB may have higher pyroelectric property in a wide temperature range from room temperature (RT) up to T_d, according to the working principle of the two main classes of pyroelectric materials described above. Lead-free BNT-based solid solutions with MPB composition have been designed, synthesized, and characterized for piezoelectric applications and are considered to be one of the potential candidates to replace PZT piezoelectric ceramics.[6–9] However, there is much less study on its pyroelectric property,[10,11] especially, no reports in the literature regarding the role of T_d on pyroelectric property up to date. Abe *et al.*[10] reported the pyroelectric property of MnO_2 doped BNT-0.06$BaTiO_3$ (BNBT-6) ceramics, and the pyroelectric coefficient p is $0.035\ \mu C/cm^2\,°C$ at RT. Lau *et al.*[11] studied the pyroelectric properties of BNT-$Bi_{0.5}K_{0.5}TiO_3$ and $K_{0.5}Na_{0.5}NbO_3$-based ceramics and discovered that BNT-$Bi_{0.5}K_{0.5}TiO_3$ ceramics show excellent pyroelectric properties ($p = 0.036\ \mu C/cm^2\,°C$) compared with $K_{0.5}Na_{0.5}NbO_3$-based ceramics and PZT at RT.

Among the reported BNT-based systems, $(1-x)(Bi_{0.5}Na_{0.5})TiO_3$-$xBaTiO_3$ (BNT-BT) with $x = 0.06$–0.07 near the MPB has been well studied because of its improved electrical properties. However, $Ba(Zr,Ti)O_3$ ceramics with ~5% Zr content has demonstrated better piezoelectric properties than that of $BaTiO_3$.[12] Peng *et al.* also reported that adding $BaZr_{0.058}Ti_{0.942}O_3$ into BNT instead of $BaTiO_3$ improved piezoelectric properties.[13] In addition, the substitution of Zr^{4+} for Ti^{4+} enhances structural lattice distortion and results in larger dipole moment inside the unit cell and smaller relative

a)Electronic mail: binyang@hit.edu.cn
b)Electronic mail: stzhang@mail.nju.edu.cn

dielectric permittivity, both are beneficial to improve pyroelectric property.[14] Therefore, We anticipate that BNT-Ba(Zr,Ti)O_3 ceramics may possess higher pyroelectric property than that of BNT-BT ceramics, yet no relevant work has been reported in the literature. In this work, $(1-x)Bi_{0.5}Na_{0.5}TiO_3$-$xBaZr_{0.055}Ti_{0.945}O_3$ (BNT-BZT) ($x = 0$, 0.03, 0.05, 0.06, 0.07, 0.08, 0.09, 0.10, and 0.12) ceramics were prepared, and their crystal structure and pyroelectric property were investigated. In particular, the effects of both MPB and T_d on pyroelectric behavior have been investigated systematically.

Reagent grade Bi_2O_3 (≥99.9%), Na_2CO_3 (≥99.8%), TiO_2 (≥99.0%), $BaCO_3$ (≥99.0%), and ZrO_2 (≥99.0%) were used as the starting raw materials and $(1-x)$BNT-xBZT ceramic specimens were prepared by two-step solid state reaction method. The precursors BNT and BZT were calcined at 820 °C and 1200 °C, respectively, for 2 h in air. Both calcined BNT and BZT powder were then mixed at specified proportion and sintered at 1130 °C for 5 h in covered alumina crucibles. The crystal structure of the sintered ceramics was determined by x-ray diffraction (XRD) with a Cu Kα radiation.

Prior to electrical measurements, ceramic disks were ground to approximately 500 μm in thickness and polished to get smooth and parallel surfaces. After polishing, the surfaces of the disks were covered with a thin layer of silver paste and fired at 550 °C for 30 min. The electrode specimens were poled in silicone oil at room temperature under a field of 5–7 kV/mm for 15 min. Temperature dependence of dielectric properties were measured on poled ceramics using a LCR meter (Agilent, E4980A) from RT to 250 °C with frequencies varying from 1 kHz to 100 kHz. The pyroelectric current measurements were carried out by using a Keithley 4200SCS with a standard short circuit method as a function of temperature at a constant heating rate of 5 °C/min. The sample temperature was controlled within 0.1 °C.

Figure 1 provides the XRD patterns of $(1-x)$BNT-xBZT ($0 \le x \le 0.12$) ceramics. All samples exhibit typical characteristics of a single-phase perovskite structure. Detailed XRD patterns in the 2θ range of 38°–48° are plotted in the inset of Fig. 1. As can be seen from Fig. 1, for compositions with $x < 0.06$, there is a shoulder located on the left of the (111) diffraction peak, this shoulder gradually decreases with increasing x and finally disappears when x reaches 0.10. On the other hand, for composition with $x < 0.06$, there are no observable (200) peak splitting, indicating that samples with these compositions have a pure rhombohedral symmetry. When $x > 0.09$, (002) and (200) peaks appear simultaneously, as presented in the inset, demonstrating pure tetragonal symmetry. Based on the above XRD data, the $x = 0.06$–0.09 ceramics have a mixture of rhombohedral and tetragonal phases, i.e., the rhombohedral-tetragonal MPB locates in the range of $x = 0.06$–0.09.

For BNT-based ceramics, the depolarization temperature T_d, which is well below the temperature of maximum permittivity T_m, is the most important limiting temperature for a pyroelectric detector. Figure 2 shows the temperature-dependent of relative free permittivity $\varepsilon_{33}^T/\varepsilon_0$ and loss tangent tanδ of poled $(1-x)$BNT-xBZT ($0 \le x \le 0.12$) ceramics from RT to 250 °C, measured at 1 kHz. As shown in Fig. 2, on the rhombohedral side, T_d determined from the peak of loss tangent of poled samples shifts to higher temperature compared to pure BNT, but for composition near the MPB, T_d shifts greatly to lower temperatures. On the tetragonal side, T_d tends to increase with composition. For all investigated compositions, the relative free permittivity $\varepsilon_{33}^T/\varepsilon_0$ of poled samples showed very little frequency dispersion below T_d, indicating that field-induced ferroelectric ordering occurred. Reorientation of ferroelectric domains induced by increasing temperature will contribute to pyroelectric effect. When the ceramic samples are heated to T_d, AFE phase appears and the phase transformation from FE to AFE results in an abrupt change in polarization.

The temperature-dependent pyroelectric current densities $J(T)$ of poled $(1-x)$BNT-xBZT ($0 \le x \le 0.12$) ceramic samples are plotted in Figs. 3(a) and 3(b). As shown in Fig. 3, $J(T)$ of all compositions shows a single sharp peak around the depolarization temperature T_d in the whole investigated temperature range. This peak corresponds to the ferroelectric-antiferroelectric phase transition around T_d for poled samples, at which most dipoles are reorientated so that significant pyroelectric current is released. The pyroelectric

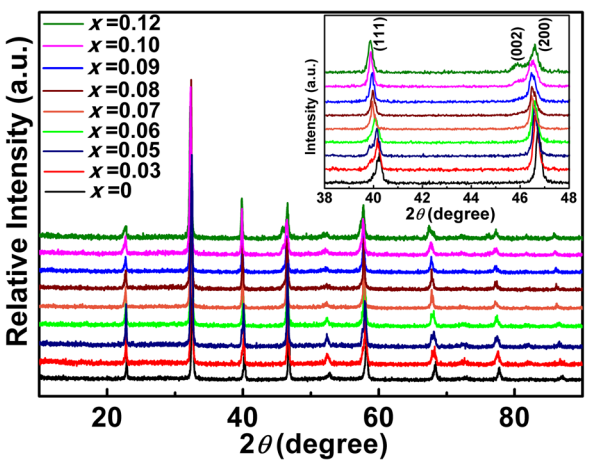

FIG. 1. XRD patterns of $(1-x)$BNT-xBZT ($0 \le x \le 0.12$) ceramics.

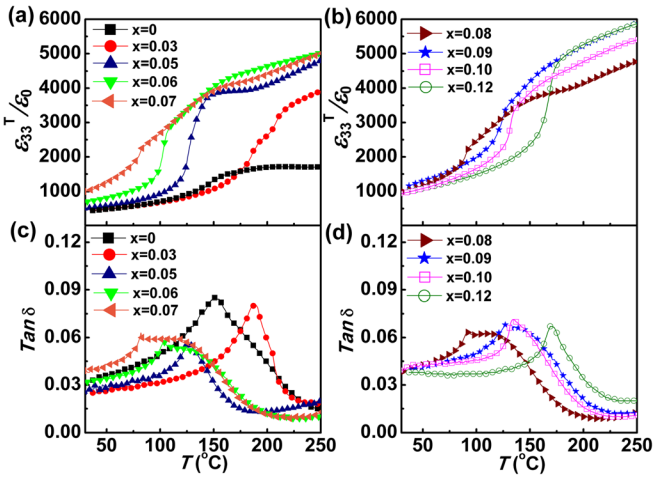

FIG. 2. (a)–(d) Temperature dependence of the relative free permittivity $\varepsilon_{33}^T/\varepsilon_0$ and loss tangents tan δ at 1 kHz in temperature range of RT−250 °C for poled $(1-x)$BNT-xBZT ($0 \le x \le 0.12$) ceramics.

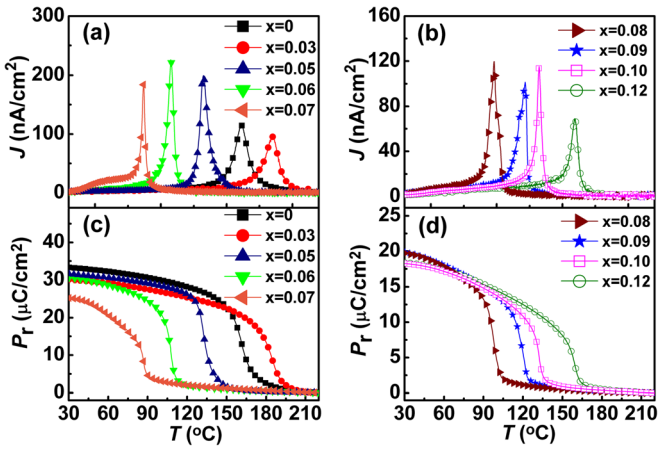

FIG. 3. (a) and (b) The temperature-dependent pyroelectric current density $J(T)$ of poled $(1-x)$BNT-xBZT $(0 \le x \le 0.12)$ ceramics; (c) and (d) the remanent polarization P_r calculated by integrating the $J(T)$ for $(1-x)$BNT-xBZT $(0 \le x \le 0.12)$ ceramics.

coefficient p is defined as the derivative of spontaneous polarization P_r with respect to temperature T, as shown by[15–19]

$$p = \frac{dP_r}{dT} = \frac{J(T)}{dT/dt}. \quad (1)$$

The value of P_r is obtained by integration of the $J(T)$ according to the following equation:[15–19]

$$P_r = \int_{T_1}^{T_2} \frac{J(T)}{dT/dt} dT, \quad (2)$$

where $J(T)$ is the pyroelectric current density, dT/dt is heating rate, and T_1 and T_2 are the lower and the upper temperatures, respectively. According to Eq. (2), temperature-dependent remnant polarization P_r of the $(1-x)$BNT-xBZT $(0 \le x \le 0.12)$ ceramics has been calculated by integrating $J(T)$ and shown in Figs. 3(c) and 3(d). For all compositions, P_r decreases suddenly when the temperature reaches T_d and almost disappears above T_d, which is consistent with the result obtained by measuring the P-E hysteresis loops. The values of P_r for all samples calculated by integrating $J(T)$ from 30 °C to 220 °C are slightly less than the values obtained from P-E hysteresis loops measured at RT. The values of P_r for the MPB composition of $x = 0.07$ acquired by the two methods are 25.2 μC/cm^2 and 29.2 μC/cm^2, respectively.

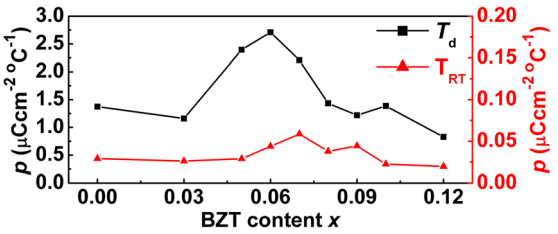

FIG. 4. The composition-dependent pyroelectric coefficient p of $(1-x)$BNT-xBZT $(0 \le x \le 0.12)$ ceramics at room temperature and near T_d.

The pyroelectric coefficient p of $(1-x)$BNT-xBZT $(0 \le x \le 0.12)$ ceramics has been calculated from $J(T)$ using Eq. (1) as a function of temperature. Figure 4 shows the composition-dependent pyroelectric coefficient p at RT and near T_d for all ceramic samples. As we can see from Fig. 4, the MPB compositions ($x = 0.06$ and 0.07) display higher pyroelectric coefficient in a wide temperature range from RT to T_d. The highest p value of $\sim$0.057 μC/cm^2 °C at RT is achieved at $x = 0.07$, which is about twice the value observed in pure BNT ceramics (0.029 μC/cm^2 °C) and much higher than reported values of other lead-based and lead-free ceramics, as listed in Table I.[11,20] The maximum pyroelectric coefficient p for $x = 0.06$ and 0.07 are 2.67 μC/cm^2 °C at 107 °C ($\sim T_d$) and 2.21 μC/cm^2 °C at 87 °C ($\sim T_d$), respectively. These values are about 8 times higher than that of MnO_2 doped BNBT-6 and 13 times higher than that of BNKT-18 ceramics near 80 °C ($\sim T_d$).[10,21] The high pyroelectric coefficient of the MPB composition in a wide temperature range from RT to T_d can be explained as the following: at lower temperatures, the pyroelectric coefficient mainly arises from ferroelectric domain reorientation and the MPB plays a positive role in improving the pyroelectric property. When the temperature increases from RT to T_d, the effect of phase transition increases. At T_d, antiferroelectric phase appears, in which the antiparallel dipoles neutralize each other leading to net zero polarization. Thus, the transformation from ferroelectric to antiferroelectric phases results in an abrupt change in polarization, which causes significant increase of the pyroelectric coefficient.

Pyroelectric figures of merit (FOMs), defined as $F_i = p/c_v$, $F_v = p/c_v\varepsilon_0\varepsilon_r$, and $F_d = p/(c_v\sqrt{\varepsilon_0\varepsilon_r \tan\delta})$, where c_v is the volume specific heat and ε_0 is the permittivity of free space, are very important for the pyroelectric infrared detector applications. For the $x = 0.07$ ceramics, when $c_v = 2.81$ J/cm^3 °C,[10] the RT FOMs are: $F_i = 203$ pm/V, $F_v = 0.022$ m^2/C, and $F_d = 10.5$ μPa$^{-1/2}$, which are superior to other lead-based and lead-free ceramics.[11,20] For

TABLE I. Pyroelectric properties of the BNT-BZT and other ferroelectric ceramics.

Material/temperature	p (μC/cm^2 °C)	F_i ($\times 10^{-10}$ m/V)	F_v ($\times 10^{-2}$ m^2/C)	F_d ($\times 10^{-5}$ Pa$^{-1/2}$)	Ref.
$x = 0.07$/RT	0.057	2.03	2.18	1.05	This work
$x = 0.07$/50 °C	0.20	7.33	6.60	3.36	This work
$x = 0.07$/87 °C	2.21	...	...	...	This work
BNT-0.07BT/RT	0.044	1.58	1.44	0.78	This work
BNKBT/RT	0.0325	1.95	2.6	1.343	11
KNLNTS/RT	0.019	0.931	0.7	0.598	11
CSBN0.15/RT	0.036	1.72	2.08	1.15	20
PZT/RT	0.0414	1.415	0.8	0.901	11

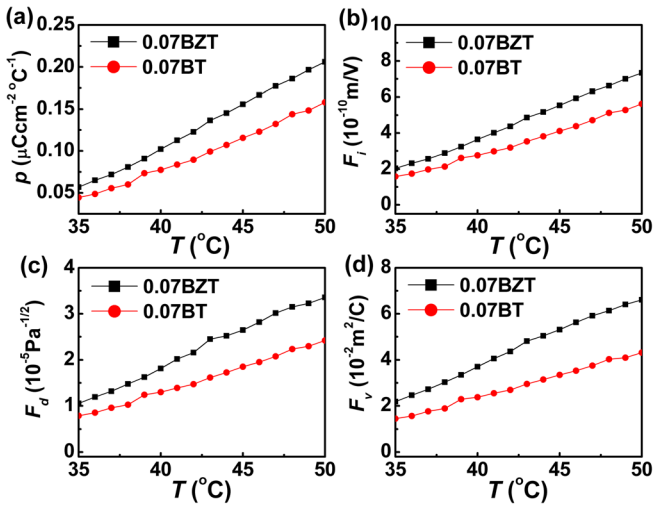

FIG. 5. Pyroelectric coefficient p and figures of merit of F_i, F_v, and F_d as a function of temperature for BNT-0.07BZT and BNT-0.07BT ceramics.

comparison, the values of p, F_i, F_v, and F_d for $x = 0.07$ ceramics at room temperature are listed in Table I.

An important feature of high-performance pyroelectric materials in pyroelectric infrared detector applications is their applicability in a wide temperature range. Figure 5 shows the temperature dependence of p, F_i, F_v, and F_d for BNT-BZT ceramics with $x = 0.07$ in a temperature range from 35 to 50 °C. Obviously, the values of p and FOMs of F_i, F_v and F_d display remarkable increase with the increasing temperature, especially the value of p from 0.057 μC/cm^2 °C at 35 °C increases to 0.206 μC/cm^2 °C at 50 °C, which is attributed to the ferroelectric-antiferroelectric phase transition. For understanding the effect of Zr-substitution on the pyroelectric properties of BNT ceramics, the same parameters of BNT-0.07BT ceramics are shown in Figure 5. As one can see that the substitution of Zr^{4+} for Ti^{4+} ion improved the pyroelectric properties, which may be explained from the viewpoint of lattice structure distortion. For the BNT-0.07BT/BZT, the c/a ratio can be a measure for the degree of distortion. The c/a value is 1.0124 for the BNT-0.07BZT ceramics, which is larger than 1.0071 for the BNT-0.07BT ceramics, i.e., the substitution of larger Zr^{4+} ($R_{Zr}{}^{4+} = 0.72$ Å) for Ti^{4+} ($R_{Ti}{}^{4+} = 0.605$ Å) enhances structural distortion. Therefore, the BNT-0.07BZT ceramic possesses superior pyroelectric properties.

In summary, $(1-x)$BNT-xBZT with $(0 \le x \le 0.12)$ ceramic samples were prepared, and their crystal structure and pyroelectric properties were studied in detail. The MPB between rhombohedral and tetragonal phases was determined to be in the range of $x = 0.06$–0.09 by XRD. Compared with other lead-based/lead-free ceramics, the MPB composition ceramic with $x = 0.07$ exhibits superior pyroelectric properties in a wide temperature range from RT to T_d with pyroelectric coefficient of 0.059 μC/cm^2 °C and the figures of merit of $F_i = 203$ pm/V, $F_v = 0.022$ m^2/C, and $F_d = 10.5$ μPa$^{-1/2}$ at room temperature and the highest pyroelectric coefficient of 2.21 μC/cm^2 °C was obtained near T_d. Both the MPB and ferroelectric-antiferroelectric phase transition play positive role in improving the pyroelectric properties. Our results indicate that the BNT-0.07BZT lead-free ceramic is a superior pyroelectric material, which opens the door for more sensitive environmental friendly temperature sensors and thermal imaging applications.

This research was supported by the National Key Basic Research Program of China (973 Program) under Grant No. 2013CB632900, the Key Technologies R&D Program of China under Grant No. 2013BAI03B06, the National Nature Science Foundation of China (Nos. 10704021, 51102062, and 11174127), the Key Scientific and Technological Project of Harbin (Grant No. 2009AA3BS131), the Postdoctoral Foundation of Heilongjiang Province (Grant No. LBH-Z10147), and the Fundamental Research Funds for the Central Universities (Grant No. HIT. NSRIF. 2011011).

[1]G. Z. Zhang, S. L. Jiang, Y. K. Zeng, Y. Y. Zhang, Q. F. Zhang, and Y. Yu, J. Am. Ceram. Soc. **92**, 3132 (2009).
[2]Q. F. Zhang, M. Y. Fan, S. G. Jiang, T. Q. Yang, and X. Yao, Appl. Phys. Lett. **101**, 062906 (2012).
[3]J. Y. Lian and T. Shiosaki, Ferroelectrics **137**, 89 (1992).
[4]C. P. Shaw, S. Gupta, S. B. Stringfellow, A. Navarro, J. R. Alcock, and R. W. Whatmore, J. Eur. Ceram. Soc. **22**, 2123 (2002).
[5]Y. Saito, H. Takao, T. Tani, T. Nonoyama, K. Takatori, T. Homma, T. Nagaya, and M. Nakamura, Nature (London) **432**, 84 (2004).
[6]T. Takenak, K. Maruyama, and K. Sakata, Jpn. J. Appl. Phys. Part 1 **30**, 2236 (1991).
[7]A. Sasaki, T. Chiba, Y. Mamiya, and E. Otsuki, Jpn. J. Appl. Phys. Part 1 **38**, 5564 (1999).
[8]X. X. Wang, X. G. Tang, and H. L. W. Chan. Appl. Phys. Lett. **85**, 91 (2004).
[9]A. B. Kounga, S. T. Zhang, W. Jo, T. Granzow, and J. Rödel, Appl. Phys. Lett. **92**, 222902 (2008).
[10]J. Abe, M. Kobune, T. Nishimura, T. Yazaw, and Y. Nakai, Integr. Ferroelectr. **80**, 87 (2006).
[11]S. T. Lau, C. H. Cheng, S. H. Choy, D. M. Lin, K. W. Kwok, and H. L. W. Chan, J. Appl. Phys. **103**, 104105 (2008).
[12]Z. Yu, C. Ang, R. Guo, and A. S. Bhalla, J. Appl. Phys. **92**, 1489 (2002).
[13]C. Peng, J. F. Li, and W. Gong, Mater. Lett. **59**, 1576 (2005).
[14]N. Sawangwan, J. Barrel, K. Mackenzie, and T. Tunkasiri, Appl. Phys. A **90**, 723 (2008).
[15]A. G. Chynoweth, J. Appl. Phys. **27**, 78 (1956).
[16]A. M. Glass, Phys. Rev. **172**, 564 (1968).
[17]R. L. Byer and C. B. Roundy, Ferroelectrics **3**, 333 (1972).
[18]S. T. Liu and D. Long, Proc. IEEE **66**, 14 (1978).
[19]J. P. Dougherty and R. J. Seymour, Rev. Sci. Instrum. **51**, 229 (1980).
[20]J. Zhang, X. L. Dong, F. Cao, S. B. Guo, and G. S. Wang, Appl. Phys. Lett. **102**, 102908 (2013).
[21]Q. F. Zhang, S. L. Jiang, and T. Q. Yang, J. Electroceram **29**, 8 (2012).